Available online at www.sciencedirect.com

ScienceDirect

Procedia CIRP 31 (2015) 94 – 99

www.elsevier.com/locate/procedia

15th CIRP Conference on Modelling of Machining Operations

Machining Process Simulations with Smoothed Particle Hydrodynamics

Fabian Spreng[a], Peter Eberhard[a,*]

[a]*Institute of Engineering and Computational Mechanics, University of Stuttgart, Pfaffenwaldring 9, 70569 Stuttgart, Germany*

[*] Corresponding author. Tel.: +49-711-68566388; fax: +49-711-68566400. *E-mail address:* peter.eberhard@itm.uni-stuttgart.de

Abstract

Because of its meshless nature, the Smoothed Particle Hydrodynamics (SPH) method is a promising alternative to well-established mesh-based simulation techniques like the Finite Element Method when investigating setups that are characterized by a highly dynamic behavior as well as large deformations of the initial configuration. This is typically the case for machining processes. First, a brief introduction to the basic principle of the SPH discretization formalism is provided. Second, the extensions to the original SPH solid scheme that are necessary to model the process of metal cutting in an appropriate way, i.e., to take into account, among other things, the thermal aspects of the problem, are introduced. Besides, emphasis is placed on the local adaptive resolution strategy that has been developed and helps to improve the accuracy of the simulation results while reducing the required computational cost at the same time. The main focus of this paper is on the capability of the extended SPH solid model to describe real machining processes in simulations. Here, we demonstrate that the employed discretization method is able to reproduce the behavior of a processed workpiece observed in experiments by analyzing and, subsequently, assessing the obtained simulation results in terms of chip morphology, stress and temperature distribution, as well as cutting force. For validation purposes, we compare the results found from both simple two- and fully three-dimensional simulations with experimental data for steel C45E.

Peer-review under responsibility of the International Scientific Committee of the "15th Conference on Modelling of Machining Operations

Keywords: Machining; Simulation; Smoothed Particle Hydrodynamics

1. Introduction

Machining is and will be, beyond all doubt, for a long time the most important manufacturing process. Therefore, already minor improvements made to any kind of cutting operation affect a huge number of applications at once. For this reason, it is of keen interest to both academia and industry to tap the full potentials of machining processes in terms of efficacy and efficiency. Here, simulations can make a major contribution to speed up the process of innovation and shorten development cycles by supporting necessary experiments as they are less expensive, less dangerous, and less time-consuming in preparation compared with experimental investigations. But as the cutting processes to be modeled are governed by many different phenomena that simultaneously influence the behavior of the considered machining systems, e.g. the mechanisms of energy dissipation and material separation, the development of a suitable simulation environment is a rather challenging task.

As a result of their mesh-based nature, simulation techniques such as the Finite Element Method and its derivatives suffer from several drawbacks when it comes to applications which are characterized by a highly dynamic behavior or large deformations of the initial configuration, and, with this, changes in the topology of the system. Against this background, meshless methods, which are not limited by an underlying mesh, are a promising alternative. However, also the meshless simulation techniques, for example the Smoothed Particle Hydrodynamics (SPH) method presented in [1], do not provide an out-of-the-box solution to the given problem. Instead, the SPH spatial discretization scheme has to be improved in order to achieve a simulation setup for solids that is capable of realistically representing the process of metal cutting.

The necessary modifications to the original SPH formalism, e.g. the introduction of an appropriate plasticity and fracture model, as well as a local adaptive resolution strategy, are discussed in the first part of this paper. In its second part, emphasis is placed on the validation of the capability of the enhanced SPH solid formulation to reproduce the behavior of real machined workpieces in simulations. For this purpose, the results obtained from orthogonal as well as oblique cutting simulations that have been performed by the SPH solid plugin for the particle simulation package Pasimodo [2] are analyzed in detail regarding chip morphology, stress and temperature distribution, as well as cutting force, and they are compared with experimental data.

Peer-review under responsibility of the International Scientific Committee of the "15th Conference on Modelling of Machining Operations

doi:10.1016/j.procir.2015.03.073

2. Basic Principle of Smoothed Particle Hydrodynamics

The meshless simulation technique SPH [3,4] belongs to the group of Lagrangian discretization methods. It can be used to solve partial differential equations (PDEs) [5]. For this purpose, the original system of PDEs in time and space is transformed into a set of ordinary differential equations in time only, which then can be numerically integrated with common integration schemes. This transformation process consists of the following three steps.

First, an ensemble of abstract particles, each representing a specific part of the original spatial domain, is introduced. Such an SPH particle carries all the properties of the assigned segment of the considered simulation domain, e.g. its mass and density. It is possible to eliminate the dependency on the spatial position and its derivatives in case of any PDE by taking the created particles and its convolution with the Dirac delta function.

Second, the Dirac delta function used for the spatial discretization is approximated by a kernel function. The contribution of each neighboring SPH particle to a property of the particle of interest is weighted according to the distance between these two interpolation points and the shape of the applied kernel function. That is the reason why the kernel function is often referred to as weight function. Usually, the functions used as kernels are cut off at a user-defined distance from the interpolation center – the so-called smoothing length – to save computational effort by not taking into account the relatively minor contributions from distant particles.

Third, the integral over the entire support area of a particle, which has been introduced in conjunction with the Dirac delta function in the first step, has to be replaced with a sum over all neighboring SPH particles in case of a finite number of interpolation points.

3. Smoothed Particle Hydrodynamics for Metal Cutting

The SPH discretization procedure we employ to solve the well-known Euler equations, i.e. the continuity and the acceleration equation, is based on the one proposed in [1]. For solid mechanics simulations, the Mie-Grüneisen equation of state [6] is applied to close the system of governing equations. The kernel is the Gaussian distribution with an initial smoothing length of 1.7 times the initial particle spacing Δx. In addition, the parameters α and β of the artificial viscosity term are set to values 1.0 and 2.0, respectively, and the scaling factor of the artificial stress tensor is chosen to be 0.15. With regard to the time integration, the second-order explicit Leapfrog scheme [7] is used and the maximum step size is limited by the Courant-Friedrichs-Lewy criterion [8].

Since the thermoplastic character of the processed material is of high influence on the behavior of the machined workpiece and, thus, the obtained results, the basic SPH solid formulation introduced in [1] needs to be extended to include such a response of the modeled continuum also in cutting simulations. These modifications, as well as an appropriate force model for boundary interactions and a local adaptive resolution scheme, are briefly discussed hereinafter. More detailed information on our enhanced SPH method for solid bodies can be found in [9].

3.1. Plasticity and fracture model

For the cutting simulations presented in this paper, the purely empirical Johnson-Cook flow stress model [10] is used to describe the evolution of the yield stress, which is contingent on the current level of plastic strain. To also be able to simulate the damage behavior that is observed for a real machined workpiece, the related cumulative-damage fracture model [11], too, has been implemented. Both the plasticity and the fracture model proposed by Johnson and Cook are not only primarily dependent on the actual plastic strain, but also on the strain rate and the temperature of the material. This dependency on the temperature allows to reproduce the thermoplastic response of the processed matter in simulations.

In order to take into account the decrease in the stress level caused by the incurred material damage, a scalar parameter D is defined for each SPH particle. It is used to replace the particle's original stress tensor $\boldsymbol{\sigma}$, i.e., the one found in case that the process of material damage is neglected, by the damaged stress tensor $\boldsymbol{\sigma}_\mathrm{D}$ [12], which is defined through $\boldsymbol{\sigma}_\mathrm{D} = (1 - D)\,\boldsymbol{\sigma}$. Choosing an initial value of 0 for D means that the represented domain of material is in pristine condition at the beginning of the simulation. Subsequently, the damage parameter is allowed to grow under both tensile and compressive loading until a maximum of 1 is reached. A value of 1 for the parameter D indicates that an SPH particle suffers from total damage and, according to that, that material fracture is present. The set of parameter values for the Johnson-Cook material model that is applied to simulate the behavior of engineering steel C45E is given in Table 1. Here, A, B, C, n, m, and D_1 to D_5 are material-dependent coefficients. Besides, $\dot{\varepsilon}_{\mathrm{pl},0}$ denotes the reference equivalent plastic strain rate, T_ambient represents the ambient temperature, and T_melt is the melting temperature. Unless otherwise stated, all material-related parameters used in the present paper are results of measurements conducted by the Institute for Machine Tools, University of Stuttgart.

Table 1. Parameter values for the Johnson-Cook plasticity and fracture model.

parameter	value	unit
A	$5.53 \cdot 10^8$	$\mathrm{N/m^2}$
B	$6.00 \cdot 10^8$	$\mathrm{N/m^2}$
C	$1.34 \cdot 10^{-2}$	–
n	$2.34 \cdot 10^{-1}$	–
m	1.00	–
T_melt	1753.15	K
T_ambient	293.15	K
$\dot{\varepsilon}_{\mathrm{pl},0}$	$1.00 \cdot 10^{-3}$	1/s
D_1	0.06	–
D_2	3.31	–
D_3	−1.96	–
D_4	$1.80 \cdot 10^{-3}$	–
D_5	0.58	–

3.2. Boundary force model

With regard to the interaction of the SPH particles with the triangular surface mesh representing the tool geometry, a penalty approach is taken. The penalty force function proposed in [13] is quite similar to the original Lennard-Jones potential [14], but does not tend to infinity as the distance between a

particle and a triangle goes to zero. In this model, H denotes the interaction range, i.e., the maximum distance up to which a contact between a particle and a triangle occurs. It is chosen as $H = \Delta x$. The resulting force points in the direction of the triangle's normal and changes with increasing distance from repulsion to attraction at distance r_0. As we want only repulsive boundary forces to appear in the simulation, we choose $r_0 = H$. The stiffness scaling factor k of the model is set to be $2.1 \cdot 10^7$, which is also the maximum force value acting on the interaction partners in case of a vanishing distance. On top of that, the contact model presented in [13] includes friction based on the difference in the partners' tangential velocities. The boundary viscosity control parameter μ has a value of 0.5.

3.3. Energy dissipation and heat conduction model

During the cutting of metal, by far the largest part of applied energy is dissipated [15]. This process of energy dissipation is mainly driven by two mechanisms; the plastic deformation of the processed material (predominantly the one of the chip) and the friction between tool and workpiece. Both of them lead to an increase in the thermal and, as a consequence thereof, the internal energy of the tool and the workpiece. For this reason, it is necessary to consider the energy equation in addition to the abovementioned Euler equations as well as to track a particle's temperature in SPH cutting simulations. In case of the presented investigations, only the warming of the workpiece is taken into consideration.

Since the governing dissipative processes primarily take place in the vicinity of the tool-workpiece interface, the related increase in internal energy and, thus, temperature is localized. Because of that, heat is conducted within the solid body following Fourier's law. By modeling the process of energy transfer caused by differences in the temperature on a molecular level, it reproduces the flux of thermal energy within the considered temperature field over time and, as a result, allows to determine the temperature as well as the thermal energy at a specific point of this field at time t. Due to the fact that SPH is a universal spatial discretization method transforming PDEs into ordinary differential equations, it is also applicable to the basic equation of heat conduction. The resulting model equation for an isotropic, homogeneous solid in its SPH form that has been derived from the first law of thermodynamics while using the Finite Difference Method to improve it is provided in [16].

3.4. Local adaptive resolution strategy

The required computational effort of any SPH simulation is primarily dependent on the number of particles used for the spatial discretization of the model domain. Consequently, one seeks to minimize the overall amount of interpolation points while not or only to a small extent diminishing the accuracy of the found results. Instead of increasing the discretization level for the whole model and with it the necessary computation time, the adaptation shall be restricted to the parts that really have need for it. For this purpose, the number of SPH particles is, on the one hand, to be adaptively increased in critical areas of a simulation model. Typically, these are areas showing a low particle density and fairly inhomogeneous distributions in stress, strain, temperature, or other field variables over the structure. On the other hand, the number of interpolation points is to be decreased in domains of little interest, i.e. the ones with a high particle density and low gradients. To that end, we developed an enhanced SPH formalism that allows for such a dynamic adaptation of the discretization level of a simulated continuum at runtime by combining a local adaptive refinement technique with an appropriate coarsening algorithm.

The proposed variable resolution scheme for SPH consists of three steps. First of all, it is decided if a particle is to be adapted by checking whether a user-defined criterion is met or not. In case that the criterion is met, the SPH particle is, in a second step, split into several smaller ones or merged with some of its neighbors into a bigger one according to a prespecified pattern. Third and finally, the state variables of the new particles must be calculated either directly from the corresponding values of the original ones or by interpolating them from the values provided by their SPH neighbors.

Further details on both the theoretical background of the developed variable resolution technique and its applicability to different types of simulation scenarios covering fluid dynamics as well as solid mechanics can be found in [17]. The benefit gained from an adaptive spatial discretization when simulating machining processes is discussed in the following section. The set of parameter values for the combined refinement and coarsening algorithm used for the presented cutting simulations are given in Table 2.

Table 2. Parameter values for the spatial adaptivity algorithm.

parameter	value
allowed number of refinement steps per particle	1
refinement pattern (2D / 3D)	square / cubical
dispersion of refinement pattern ε	0.5
smoothing length multiplication factor α	0.85
strategy for velocity calculation	cloning
distribution of mass along particles of same refinement cell	unequal
allowed number of coarsening steps per particle	1
coarsening pattern (2D and 3D)	family-based
desired number of particles to be merged (2D / 3D)	4 / 8
tolerance limit for Newton-Raphson method	$1 \cdot 10^{-6}$
maximum number of steps for Newton-Raphson method	20
minimum number of time steps since last refinement	10

4. Results

In the second part of the present paper, the capability of the proposed SPH solid formulation to model the process of metal cutting is now investigated. For this purpose, several two- and three-dimensional simulations of both orthogonal and oblique machining processes have been performed. In this section, their results are analyzed as well as assessed in terms of chip morphology, stress and temperature distribution, as well as cutting force.

First, the more simple scenario of an orthogonal cutting process is considered. Then, the results found for fully three-dimensional simulations of an oblique cutting setup are discussed. In both cases, the shape of the cutting tool can have a significant influence on the behavior observed for the entire cutting system and, hence, the obtained results. The cutting edge of a real tool reveals deviations in its geometry from an

ideal wedge shape due to wear and manufacturing [18]. Therefore, not a tool with an ideal geometry, i.e. a wedge shape, but a more sophisticated one that takes into account the imperfections resulting from the acting wear mechanisms and the limitations of the manufacturing process is employed for the machining simulations. In [19], such a model that promises a sufficient imitation of a real slightly worn tool is found. Because of its wide application in mechanical engineering, the material used for both the conducted experiments and the performed cutting simulations is engineering steel C45E. The material properties for this type of steel at room temperature are listed in Table 3. Further information on the prepared simulation setup for cutting processes is provided in [20].

Table 3. Physical properties of engineering steel C45E at room temperature.

property	value	unit
density ρ	$7.80 \cdot 10^3$	kg/m^3
Young's modulus E	$2.10 \cdot 10^{11}$	N/m^2
Poisson ratio ν	0.3	–
yield strength σ_y	$5.53 \cdot 10^8$	N/m^2
fracture strain ε_f	$1.33 \cdot 10^{-1}$	–
specific heat capacity at constant pressure c_p	460	J/kgK
thermal conductivity λ	55	W/mK

4.1. Orthogonal cutting

The fundamental machining process of orthogonal cutting [15] was first investigated using the SPH method by J. Limido and coworkers in 2007 [21]. As there exist lots of fundamental differences between their setup and the present one, e.g. static vs. adaptive spatial resolution, geometrical vs. empirical fracture model, particle- vs. triangle-based dicretization of cutting tool, no further comparison between these two models is provided in this paper.

In case that the width of cut is sufficiently larger than the depth of cut, the existence of a two-dimensional state of stress in the workpiece can be assumed and, hence, the setup becomes a planar problem [22]. That is why a two-dimensional model of an orthogonal cutting specimen can be deployed.

For the workpiece model with a length of $1.15 \cdot 10^{-2}$ m and a height of $3 \cdot 10^{-3}$ m, the SPH particles are positioned according to a structure consisting of quadratic cells with an edge length of $5.58 \cdot 10^{-5}$ m. All particles have an initial temperature of $T = T_{\text{ambient}}$ and no heat is exchanged with the environment, i.e., an adiabatic system is considered. In order to prevent the model from following an unconstrained translational motion, five additional rows of SPH particles that are fixed in space and are assigned the constant temperature T_{ambient} are attached to the bottom of the specimen. This leads to an overall number of interpolation points of about 12,000 in the initial configuration.

For a depth of cut of $6 \cdot 10^{-4}$ m and a cutting speed of 1.6 m/s, a continuous chip as depicted in Fig. 1 is separated from the workpiece in the orthogonal cutting simulation. When examining the distribution of the von Mises equivalent stress obtained from the statically discretized model, one finds that the highest level of stress, which is indicated by the red color, appears next to the tip of the gray-colored tool as well as in the primary shear zone. These zones showing a high magnitude of equivalent stress are surrounded by one of mid-level stress, which is color-coded with yellow and green. The SPH particles that are located at some distance from both the tool tip and the primary shear zone show low values of von Mises stress, as indicated by their blue color. As a consequence, high gradients in stress are found in the region of the tool cutting edge for the simulated workpiece. When considering the results shown in Fig. 1, it is important to remember that the illustrated particles only represent the interpolation points where the SPH equations of the underlying continuum model are evaluated, not domains of material.

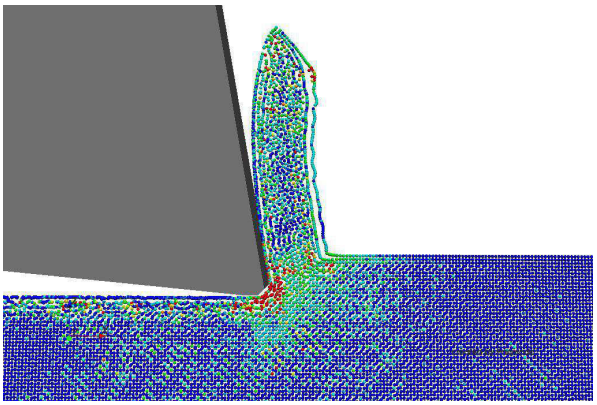

Fig. 1. Distribution of the von Mises stress found for the statically discretized SPH workpiece model (red: high stress; blue: low stress).

If the adaptive discretization technique introduced in Section 3.4 is applied to the orthogonal cutting setup, a refinement of the load-carrying particles in the different shear zones of the workpiece can be observed, see Fig. 2. While the SPH particles showing a blue color still have the initial size, the red-colored ones have been refined to be able to resolve the abovementioned high gradients in stress found for these regions. Here, a stress-based refinement criterion together with a square refinement pattern is used. For the areas of the model that have already been passed by the cutting tool, the previously refined SPH particles are adaptively coarsened when reaching a stress level that

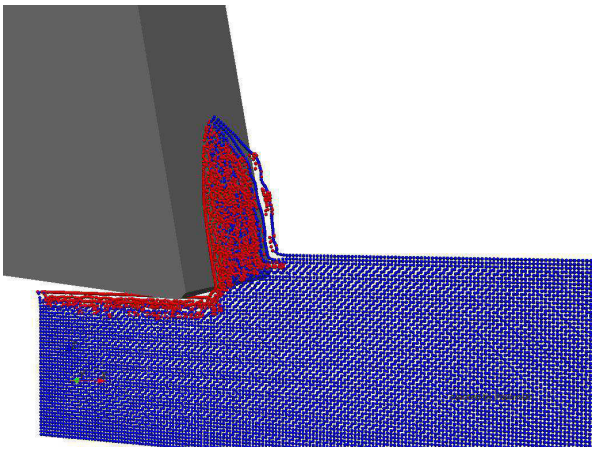

Fig. 2. Simulation result for the orthogonal cutting model obtained with the adaptive SPH method (red: refined particle; blue: original/coarsened particle).

is at least ten times lower than the specified refinement threshold value, as indicated by their blue color. For the coarsening process, a family-based strategy is employed, which pays attention to both the hierarchic structure, and the refinement and coarsening history of an adaptive particle. On this basis, it tries to merge refined particles with the same origin. A more in-depth analysis and comprehensive discussion of SPH cutting simulations with a variable spatial resolution is offered in [23].

4.2. Oblique cutting

In case of the oblique cutting scenario, a regular grid of cubical cells with the same dimensions as the one used for the orthogonal cutting model and a width of $3 \cdot 10^{-3}$ m provides the basis for the arrangement of the SPH interpolation points. In order to obtain reasonable computation times for the fully three-dimensional simulations, the particle spacing Δx, i.e. the edge length of the cuboids, is increased to $2.09 \cdot 10^{-4}$ m and, according to that, the overall number of SPH particles is approximately 14,000, which is slightly higher than the one of the two-dimensional model. Moreover, the cutting tool is rotated by 30° in comparison with the preceding configuration. All other parameters are identical to those of the orthogonal cutting process setup considered before.

Also for the three-dimensional problem, a continuous, but now asymmetrically shaped chip is separated from the workpiece as a result of the tool intrusion, see Fig. 3. When analyzing the shown distribution of equivalent plastic strain of the processed solid material, one finds that it is restricted to the chip as well as to the vicinity of the tool-workpiece interface, and, accordingly, high temperatures caused by plastic deformation appear only there. Since none but the particles that are in contact with the boundary geometry representing the cutting tool are influenced by the friction between tool and workpiece, this second primary mechanism of energy dissipation is localized in the region near the tool cutting edge. Hence, the overall maximum temperature values show up next to the interface area as can be seen from Fig. 4. For the domains of material that have already been passed by the tool geometry, the generated heat is

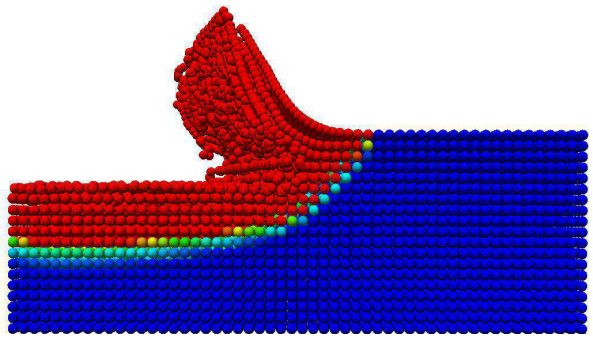

Fig. 4. Side view of the SPH oblique workpiece model (red: high temperature; blue: low temperature).

subsequently conducted within the solid body. Consequently, subjacent particle layers heat up, whereas the machined surface areas start to cool down. Comparative investigations based on the investigated SPH machining model have shown that the higher the cutting speed, the higher the level of dissipated energy due to friction and, thus, the higher the temperatures in the different shear zones; an expected relationship described in detail in [15].

In order to further assess the quality of the presented SPH oblique cutting model in terms of being capable of simulating real machining processes, an experimental reference is invoked. When examining the results given in Fig. 5, the cutting force found from experiment reveals a steep increase once the tool hits the workpiece before a steady state is reached. The simulated curve, too, is characterized by a steep rise, followed by an oscillation about a steady state at about the same level observed in case of the experimental results. Except the transition area between the steep increase just after the tool impact and the steady state, the results found from both the oblique cutting simulation and the experimental investigation are in good agreement, although the curve obtained from the simulation shows a slightly wider range of variation and a higher frequency

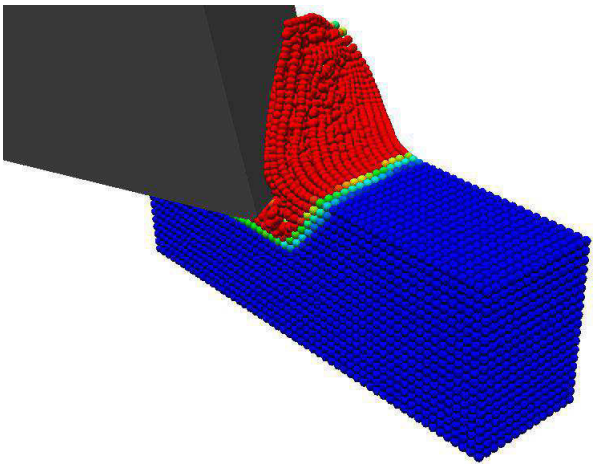

Fig. 3. Distribution of equivalent plastic strain found for the SPH oblique cutting model (red: high strain; blue: low strain).

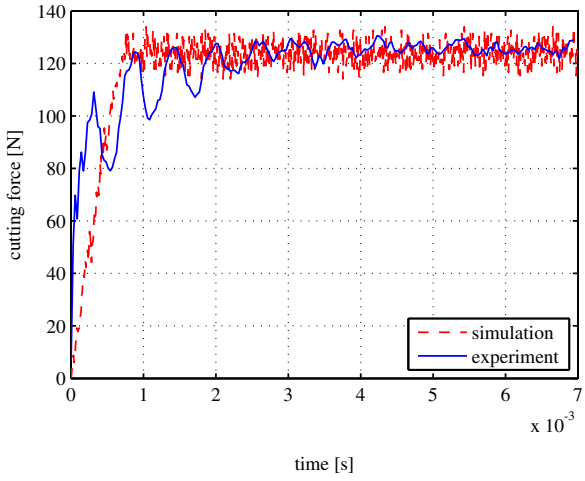

Fig. 5. Comparison of the experimental and the simulated cutting force in case of oblique cutting.

oscillation in the cutting force than the experimentally identified one. In addition to the cutting force depicted in Fig. 5, one finds such high quality of reproduction also for the two components of the thrust force acting perpendicular to it and each other.

5. Conclusion

The intention of this paper was to introduce a novel simulation environment that allows to realistically model machining operations while not experiencing any limitations from an underlying mesh being part of the employed spatial discretization scheme. The presented tool is based on the SPH particle method, a promising, since meshless simulation technique, whose basic principle was explained in Section 2. Although SPH belongs to the group of meshless discretization methods, it needs to be further improved in order to be able to correctly describe the process of metal cutting. To that end, the original SPH solid formulation has been extended to both the Johnson-Cook plasticity and the related cumulative-damage fracture model as was shown in Section 3. For the description of the interaction of the SPH particles with the cutting tool, a boundary force model that is based on a modified Lennard-Jones potential has been implemented. Not only as a result of the friction forces calculated by this model, but also due to the plastic deformation of the processed material, energy is dissipated during the cutting of metal. To model the subsequent process of transferring the heat generated by the two aforementioned dissipative mechanisms, Fourier's law in its SPH form has been added to the basic procedure. Finally, a local adaptive resolution strategy was introduced, which, on the one hand, helps to improve the accuracy of the simulation results by dynamically adjusting the spatial discretization of the particle model. On the other hand, it reduces the required computational cost at the same time.

After having presented our enhanced SPH cutting formulation, its applicability to machining operations was discussed in Section 4. In this context, the results found from simulations of orthogonal and oblique cutting processes revealed that the extended model provides a realistic behavior on both a qualitative and a quantitative level. So, the formation of a continuous chip can be observed in case of the two- as well as the three-dimensional scenario, and the highest values of von Mises equivalent stress exist next to the tool cutting edge as well as in the primary shear zone. Besides, also the maximum temperatures appear in the vicinity of the tool-workpiece interface and are shifted to higher values with increasing cutting speed. For the example of an oblique cutting process, the experimental cutting force was compared with its simulated counterpart and, that way, the capability of the extended SPH formalism to describe the behavior of a real machined workpiece in simulations was demonstrated.

Future investigations with the proposed SPH solid formulation will address, among other things, the quality of the obtained simulation results in terms of vibration behavior of the entire machining system, the influence of the tool model on the shape of the chip, as well as the correlation between the absolute level of the cutting force and the applied depth of cut.

Acknowledgements

The research leading to the presented results has received funding from the German Research Foundation (DFG) under the Priority Program SPP 1480 grant EB 195/12-3. This financial support is highly appreciated.

References

[1] Monaghan J.J., 2005. Smoothed Particle Hydrodynamics, Reports on Progress in Physics, 68(8):1703-1759.
[2] Pasimodo. *www.itm.uni-stuttgart.de/research/pasimodo/pasimodo_en.php*.
[3] Gingold R.A., Monaghan J.J., 1977. Smoothed Particle Hydrodynamics: Theory and application to non-spherical stars, Monthly Notices of the Royal Astronomical Society, 181:375-389.
[4] Lucy L.B., 1977. A numerical approach to the testing of the fission hypothesis, Astronomical Journal, 82(12):1013-1024.
[5] Liu M.B., Liu G.R., 2010. Smoothed Particle Hydrodynamics (SPH): An overview and recent developments, Archives of Computational Methods in Engineering, 17(1):25-76.
[6] Burshtein A.I., 2005. Introduction to Thermodynamics and Kinetic Theory of Matter, Berlin: Wiley-VCH.
[7] Monaghan J.J., Kos A., Issa N., 2003. Fluid motion generated by impact, Journal of Waterway, 129(6):250-259.
[8] Courant R., Friedrichs K., Lewy H., 1967. On the partial difference equations of mathematical physics, IBM Journal of Research and Development, 11(2):215-234.
[9] Spreng F., Eberhard P., 2013. The way to an enhanced Smoothed Particle Hydrodynamics formulation suitable for machining process simulations, Proceedings of the 8th International SPHERIC Workshop.
[10] Johnson G.R., Cook W.H., 1983. A constitutive model and data for metals subjected to large strains, high strain rates and high temperatures, Proceedings of the 7th International Symposium on Ballistics, 547:541-547.
[11] Johnson G.R., Cook W.H., 1985. Fracture characteristics of three metals subjected to various strains, strain rates, temperatures and pressures, Engineering Fracture Mechanics, 21(1):31-48.
[12] Benz W., Asphaug E., 1994. Impact simulations with fracture. I. Method and tests, Icarus, 107(1):98-116.
[13] Müller M., Schirm S., Teschner M., Heidelberger B., Gross M., 2004. Interaction of fluids with deformable solids, Computer Animation and Virtual Worlds, 15(3-4):159-171.
[14] Jones J.E., 1924. On the determination of molecular fields. II. From the equation of state of a gas, Proceedings of the Royal Society of London A: Mathematical, Physical and Engineering Sciences, 106(738):463-477.
[15] Boothroyd G., Knight W.A., 2006. Fundamentals of Machining and Machine Tools, 3rd edition, Boca Raton: CRC.
[16] Cleary P.W., Monaghan J.J., 1999. Conduction modelling using Smoothed Particle Hydrodynamics, Journal of Computational Physics, 148(1):227-264.
[17] Spreng F., Schnabel D., Mueller A., Eberhard P., 2014. A local adaptive discretization algorithm for Smoothed Particle Hydrodynamics, Computational Particle Mechanics, 1(2):131-145.
[18] Gaugele T., Eberhard P., 2013. Simulation of cutting processes using meshfree Lagrangian particle methods, Computational Mechanics, 51(3):261-278.
[19] Armarego E.J.A., Brown R.H., 1969. The Machining of Metals, Englewood Cliffs: Prentice-Hall.
[20] Spreng F., Eberhard P., Fleissner F., 2013. An approach for the coupled simulation of machining processes using multibody system and Smoothed Particle Hydrodynamics algorithms, Theoretical and Applied Mechanics Letters, 3(1):013005-1-7.
[21] Limido J., Espinosa C., Salaün M., Lacome J.L., 2007. SPH method applied to high speed cutting modelling, International Journal of Mechanical Sciences, 49(7):898-908.
[22] Jaspers S.P.F.C., 1999. Metal Cutting Mechanics and Material Behaviour, Dissertation, Eindhoven University of Technology.
[23] Spreng F., Schnabel D., Mueller A., Eberhard P., 2014. Smoothed Particle Hydrodynamics with adaptive discretization, Proceedings of the 9th International SPHERIC Workshop.